Asymmetric Sea Surface Salinity Response to Global Warming: "Fresh Gets Fresher but Salty Hesitates"

Hervé Douville, L. Cheng

Geophysical Research Letters

RESEARCH LETTER
10.1029/2023GL107944

Asymmetric Sea Surface Salinity Response to Global Warming: "Fresh Gets Fresher but Salty Hesitates"

H. Douville[1] and **L. Cheng**[2,3]

[1]Centre National de Recherches Météorologiques, Université de Toulouse, Météo-France, CNRS, Toulouse, France, [2]Institute of Atmospheric Physics, Chinese Academy of Sciences, Beijing, China, [3]Center for Ocean Mega-Science, Chinese Academy of Sciences, Qingdao, China

Key Points:

- Both observations and climate models evidence an amplification of the global ocean climatological contrasts in sea surface salinity (SSS)
- Yet, the "fresh gets fresher" paradigm is more robust than its salty counterpart, which is more sensitive to the ocean domain's definition
- Global SSS observations do not yet provide a strong constraint on the projected intensification of the global water cycle

Supporting Information:

Supporting Information may be found in the online version of this article.

Correspondence to:

H. Douville,
herve.douville@meteo.fr

Citation:

Douville, H., & Cheng, L. (2024). Asymmetric sea surface salinity response to global warming: "Fresh gets fresher but salty hesitates". *Geophysical Research Letters*, *51*, e2023GL107944. https://doi.org/10.1029/2023GL107944

Received 19 DEC 2023
Accepted 17 APR 2024

Author Contributions:

Conceptualization: H. Douville
Data curation: H. Douville, L. Cheng
Formal analysis: H. Douville
Investigation: H. Douville
Methodology: H. Douville
Validation: H. Douville
Visualization: H. Douville
Writing – original draft: H. Douville
Writing – review & editing: L. Cheng

Abstract Efforts to detect long-term changes in global mean evaporation minus precipitation over the ocean remain ambiguous. Here we define an ad hoc sea surface salinity index to assess the observed and simulated intensification of the freshwater flux pattern over the global ocean and, thus, of the overall water cycle. A recent salinity reconstruction shows a long-term amplification of the climatological patterns, thereby supporting the popular "fresh gets fresher, salty gets saltier" paradigm. Unlike in a previous study, no systematic underestimation of this amplification is found in the latest generation of global climate models. Yet, the "fresh gets fresher" paradigm is much more robust than its "salty gets saltier" counterpart and the proposed salinity index does not yet provide a strong constraint on the model-dependent projected intensification of the global water cycle intensification along the 21st century.

Plain Language Summary Recent changes in continental mean precipitation and evaporation remain poorly observed and thus poorly constrained in both atmospheric reanalyzes and global climate models. Here we propose a new index based on global sea surface salinity contrasts as a surrogate of changes in metric of the water cycle intensity. Overall, both observed and simulated indices support the "fresh gets fresher, salty gets saltier" paradigm, widely used to depict the overall intensification of the water cycle. Unlike in a previous study, no systematic underestimation of the observed amplification in salinity patterns is found in the latest generation of global climate models. The "salty gets saltier" response is however less robust than the "fresh gets fresher" and the proposed salinity index is not yet very useful to constrain the future intensity of the global water cycle.

1. Introduction

Both annual mean precipitation (P) and surface evaporation (E) are projected to increase in a warming climate (Douville et al., 2021). Yet, changes in terrestrial water availability (P-E over land) remain highly model-dependent (Lehner et al., 2020) and cannot be easily constrained by narrowing climate sensitivity (Elbaum et al., 2022). Observed trends in P-E are also uncertain due to limited evapotranspiration in situ measurements and large inconsistencies between multiple satellite data sets. Atmospheric reanalyzes also suffer from considerable discrepancies (Hersbach et al., 2020; Mayer et al., 2021; Robertson et al., 2016). This lack of reliable re-constructions limits our current understanding of the water cycle response to human emissions of greenhouse gases (Allan et al., 2020).

To overcome such difficulties, it is possible to focus on the oceanic component of the global water cycle (e.g., Durack et al., 2012). Ocean salinity integrates the highly variable E and P fields in both space and time, and is therefore among the best recorders of long-term changes in E-P (Cheng et al., 2020). Ocean basins provide the largest possible rain gauges on Earth, and large-scale variations in sea surface salinity (SSS, sometimes also called near-surface salinity since this is not a skin property of ocean surfaces) are shaped by both E-P patterns and oceanic circulation (Grist et al., 2016; Vinogradova & Ponte, 2013; Yu, Josey, et al., 2017; Zika et al., 2018). The former mechanism acts to create salinity contrasts, whereas ocean dynamics and small-scale vertical mixing generally act to mitigate them.

Despite a large variety of fresh and salty domain definitions, the "fresh gets fresher, salty gets saltier" (hereafter FFSS) paradigm is a widely-used summary of the overall intensification of the global water cycle (Allan et al., 2020; Bindoff et al., 2019). In a landmark study, Durack et al. (2012) inferred a +8%/°C rate of intensification from observed 1950–2000 zonal mean SSS patterns and a twofold ratio between the increase in zonal mean SSS wrt E-P contrasts simulated by global climate models (GCMs) from the third phase of the Coupled

Model Intercomparison Project (CMIP3). A few years later, *E-P* changes were assessed in four atmospheric reanalyzes, leading again to a range of increase that was much larger than in a selected GCM (Grist et al., 2016). Yet, another study, using a water mass transformation theory based on full depth salinity observations, inferred a much lower water cycle amplification of 3.0 ± 1.6%/°C over 1950–2010 (Skliris et al., 2016). Moreover, targeted numerical experiments suggested that *E-P* fluxes are not the only driver of recent changes in SSS patterns (Zika et al., 2018). To sum up, the link between SSS and *E-P* patterns seems to be sensitive to the selected data, oceanic regions and observation period.

Recently, the Institute of Atmospheric Physics (IAP) proposed a new gridded data set of observed salinity which was successfully evaluated against other available products (Cheng et al., 2020). The amplification of the climatological salinity pattern was supported by two indices simply defined as the full-depth or near-surface salinity contrast between high versus low-salinity regions. A 1960–2017 global water cycle intensification by 2.6 ± 2%/°C was inferred from the observed salinity contrast and a linear relationship between this contrast and *E-P* patterns based on CMIP5 models (Cheng et al., 2020).

Our objective here is not to reconcile these previous studies, but to propose an ad hoc salinity index, based on *E-P* rather than SSS ocean domains, and to highlight an asymmetric salinity pattern response to global warming. Taking advantage of a recent update of the IAP salinity reconstruction and of an innovative Bayesian statistical method (Ribes et al., 2021), we also try to constrain the CMIP6 projections under a high-emission scenario.

2. Data and Methods

A new version of the 0.5° resolution IAP monthly mean ocean salinity data set has been recently released (G. Li et al., 2023). It is based on a dynamic ensemble optimal interpolation (OI) scheme. To perform interpolation across data-sparse regions and intervals, the spatiotemporal covariance of salinity was estimated from historical simulations conducted as part of CMIP5, which is flow-dependent and more realistically represents the ocean variability than the widely used Gaussian covariance. The final 0–2,000 m global salinity data set has been carefully evaluated using subsample tests and independent high-resolution satellite data. It is the longest record (here 1940–2021) currently available to assess observed salinity changes. The subsample test, which samples the recent near-global-coverage data by historical data distributions, indicates that IAP reconstruction is particularly robust in describing long-term changes in salinity since ∼1960 and, thus, is most suitable for this study. The comparison with independent satellite data also indicates smaller errors compared with some of the available products (Cheng et al., 2020; G. Li et al., 2023). This is related to the integration of the ocean salinity measurements from all available instruments, the careful quality-check procedures, and the gap-filling methods.

The overall quality of subsurface salinity gridded data has been greatly improved since the beginning of the Argo measurements in 2005 mainly because of the improved data coverage. Nevertheless, even Argo-based salinity trends can disagree, especially in the subsurface North Atlantic and Southern oceans (C. Liu et al., 2020). The focus here is thus on SSS rather than on deeper ocean levels. Besides the IAP data set, two alternative SSS products have been also used: the global Ocean Reanalysis System (ORAS5; Zuo et al., 2019) from the European Center for Medium-Range Forecast (ECMWF) and a multi-observation data set from the Copernicus Marine Service (cf. Table S1 in Supporting Information S1). The ORAS5 consolidated data was forced by two successive atmospheric reanalysis and constrained by a growing amount of ocean observations. As many other ocean reanalyzes, it may suffer from marked drifts prior to the Argo period when stability and biases reduce due to the enhanced data coverage (Cheng et al., 2020; Shi et al., 2017). The early 1958–1972 period was here discarded due to much lower global mean SSS values than over the post-1970 decades.

Unlike in previous studies, including Cheng et al. (2020), we simply quantify the global SSS contrast (hereafter GSSSC) as the difference between ad hoc regions with negative ($E > P$) versus positive ($E < P$) atmospheric moisture convergence (Figure S1 in Supporting Information S1):

$$\mathrm{GSSSC} = \frac{1}{A_{E>P}} \int_{E>P} \mathrm{SSS} dA - \frac{1}{A_{E<P}} \int_{E<P} \mathrm{SSS} dA \quad (1)$$

Note that the $E > P$ and $E < P$ domains can be either "static" (based on the *E-P* annual mean climatology) or "dynamic" (i.e., based on time-varying monthly mean *E-P* fields). In both cases, the $E = P$ isoline is derived from

the latest ECMWF global atmospheric reanalysis (ERA5, Hersbach et al., 2020, 2023). Despite the lack of direct observations and data assimilation for precipitation and evaporation over the global ocean, we thus assume that the ERA5 atmospheric moisture convergence is accurate enough to delineate our two contrasted oceanic domains. Yet, we remain cautious about the quantification of the *E-P* contrast (Mayer et al., 2021) so that we will focus on GSSSC as a proxy for this contrast in the continuation of the study.

Beyond the IAP and ERA5 data sets, the 1850–2022 HadCRUT5 ensemble reconstruction of the global mean surface temperature (hereafter GMST)—a combination of near-surface air temperature over land and sea ice and of sea surface temperature (SST) over the ocean—is also used as a surrogate for the observed global mean surface air temperature (GSAT).

Moving to CMIP6 climate simulations, both historical (1850–2014) and 21st century (2015–2100) simulations from a subset of 31 models providing monthly outputs for all requested variables have been considered. The SSP5-8.5 high emission scenario was selected in order to maximize the signal to noise ratio, thus enabling the use of only one realization for each model. The global warming, as well as the global ocean contrast in *E-P* and SSS have been diagnosed from raw model outputs, without spatial interpolation onto a common grid (unlike for maps of the multi-model ensemble statistics shown in Supporting Information S1). The general pattern of the observed ocean salinity climatology was shown to be captured by most CMIP6 models in spite of an increased fresh bias in surface salinity compared to the previous generation of GCMs (Y. Liu et al., 2022).

Regarding the statistical method, we use the Kriging for Climate Change (KCC, 2023) toolbox developed by Ribes et al. (2021) and Qasmi and Ribes (2022), and already applied in a very similar way by Douville et al. (2022) or Douville and Willett (2023). It is based on Bayesian statistics where a prior distribution, $\pi(x)$, of the forced GSSSC response to anthropogenic forcings is derived from raw model outputs and constrained directly with "observations" (here both GMST from HadCRUT5 and GSSSC from IAP). The *prior* is estimated using a Generalized Additive Model and a simple Energy Budget Model (for more details, see supplementary materials from Ribes et al., 2021). The posterior distribution is obtained by assuming that observations, y, can be described as: $y = \mathcal{H}x + \varepsilon$, where $\mathcal{H}$ is a pseudo-observation operator allowing to extract the part of x observed in y, and ε represents both internal variability and observational errors. Since $\pi(x)$ and ε are supposed to follow normal distributions, the posterior can be easily derived using the Gaussian conditioning theorem. Such a bivariate application of KCC has been tested successfully with pseudo-observations (Dutot & Douville, 2023; Qasmi & Ribes, 2022) and accounts for the covariability between the two observational constraints. Finally, it should noted that KCC is usually based on absolute anomalies (here in PSU) and is thus not sensitive to potential model biases or uncertainties in the observed baseline climatology.

3. Results

We first compare the annual mean climatologies derived from the three SSS products over the common 1995–2014 period (Figure S1 in Supporting Information S1). This "present-day" period will be also used to derive annual mean anomalies in the continuation of the study. The climatological patterns are quite similar among the three salinity products and are spatially consistent with the ERA5 *E-P* climatology estimated over the same 20-year period (as highlighted by the $E = P$ isoline). In line with previous studies, large salinity values are generally found in the subtropics, where E exceeds P. Conversely, low salinity levels are predominant over the Inter-Tropical Convergence Zone and in the high latitudes, where P exceeds E.

Beyond the climatological patterns, the multi-decadal SSS variations have also been explored after spatial aggregation over the two complementary *E-P* domains used in Equation 1 and first derived from the ERA5 climatology (Figures S2a and S2b in Supporting Information S1). The absolute salinity values are stronger in IAP compared to the two other data sets. Yet, and as expected from the FFSS paradigm, both OI data sets indicate an increasing salinity in the oceanic domain where the *E-P* climatology is positive ($E > P$) and a decreasing salinity in the other domain ($E < P$). As a result, the GSSSC index (Figure S2c in Supporting Information S1) shows an apparent though not monotonic increase of 0.08 PSU per century over the available 1940–2022 period.

The suitability of the GSSSC index to depict recent and future changes in the oceanic water cycle is well supported by the strong inter-model relationship between *E-P* changes as defined in Equation 1 over the $E > P$ and $E < P$ domains, respectively (Figure S3 in Supporting Information S1). As expected, this relationship is however

stronger when using monthly time-varying $E = P$ isolines ($R^2 = 0.96$) rather than an annual mean climatology ($R^2 = 0.58$) to delineate the contrasted ocean domains.

The fact that the GSSSC index does not depend on arbitrary salinity thresholds or latitudinal boundaries does not necessarily imply that the index is less influenced by ocean transport or other confounding factors. Yet, the wider the domains are and the greater is the relative influence of freshwater fluxes compared to ocean dynamics. The link between relative changes in *E-P* versus SSS over the two contrasted domains (Figures S4a and S4b in Supporting Information S1) is partly model-dependent so that the CMIP6 inter-model relationship is not as strong as in Durack et al. (2012) or Cheng et al. (2020) as assessed from previous generations of GCMs. We however claim that a domain definition based on the sign of *E-P* is easier to interpret in terms of atmospheric horizontal water transport and overall water cycle intensity. This is further supported by a more straightforward link with the projected global warming across CMIP6 models (Figures S4c and S4d in Supporting Information S1). Our results therefore highlight the potential sensitivity of previous similar studies to the salinity index definition and call for a trade-off: the selected index should be both sensitive to the magnitude of the projected global warming and relevant as a metric of the water cycle intensity, at least above the global ocean.

In qualitative agreement with previous studies based on alternative salinity indices, the GSSSC evolution reveals a long-term amplification of the global SSS pattern in the two OI data sets based on observations only, although the expected increase of salinity over the $E > P$ domain is less clear (Figure S2 in Supporting Information S1). The annual mean time series are remarkably similar over the 1993–2021 overlapping period despite the fact that the Copernicus multivariate algorithm combines in situ salinity measurements with satellite SST and SSS retrievals from multiple satellite platforms, such as the Soil Moisture Active Passive and the Soil Moisture Ocean Salinity instruments. In contrast, no clear positive trend appears in the ORAS5 global ocean reanalysis. Such a discrepancy may arise from multiple reasons, including changes in the observation system and/or in the quality of the atmospheric forcings. Contrasted *E-P* climatologies between ERA5 and the former ECMWF reanalysis used to drive ORAS5 may also play a role through the static definition of the two ocean domains.

To mitigate this issue, all time series have been recomputed using a monthly mean time-varying, rather than fixed climatological, *E-P* mask. The resulting Figures 1a–1c compares well with Figure S2 in Supporting Information S1, but shows an even stronger consistency between the IAP and Copernicus multi-observation data sets. Moreover, the ORAS5 global ocean reanalysis now also shows a slightly increasing GSSSC index, despite a year-to-year variability which remains inconsistent with the OI data sets. Because of the well-known limitations of ocean reanalyzes (Wang et al., 2023; Yu, Jin, et al., 2017) and consistent variations of our two OI products, we are fairly confident in the IAP GSSSC index, at least since 1960 when the estimated sampling errors suggest a reliable reconstruction (Cheng et al., 2020). As a dipole, this index is likely to be less sensitive to systematic errors in absolute salinity than basin-scale averages. The long-term GSSSC increase shown in Figure 1c is qualitatively consistent with the parallel increase of the corresponding *E-P* contrast in the ERA5 reanalysis (Figure 1f). The increasingly salty domain shows a clear increase in *E-P*, whereas the freshening domain reveals a dominant decrease (although less clear in ORAS5), thus further supporting the FFSS paradigm.

If we assess the correlation between the raw annual mean IAP and ERA5 timeseries as a measure of the consistent evolution of the global salinity and *E-P* contrast respectively, the obtained 0.54 positive value is entirely explained by common positive linear trends on top of inconsistent year-to-year fluctuations (−0.03 correlation after linear detrending). This apparent inconsistency may arise from multiple reasons, including a relatively weak influence of freshwater fluxes on surface salinity at monthly to interannual timescales associated with a dominant contribution of the ocean dynamics to the SSS budget (Vinogradova & Ponte, 2013), but also deficiencies in the ERA5 reanalyzes where the water budget is not closed and changes in the observation system can lead to non-physical hydrological variations (Hersbach et al., 2020; Mayer et al., 2021). Another possible reason is the sampling of salinity observations, which results in less reliable reconstruction in representing monthly to interannual variations of SSS (with signal to noise ratio typically less than 2) than decadal-to-multidecadal variations (Cheng et al., 2020).

By design, the water budget is perfectly closed in CMIP6 models. Moreover, the high-frequency ocean-atmosphere coupling (typically every 3 hr) ensures the physical consistency of the *E-P* and SSS variability. Figure 2 shows a scatterplot of correlations showing how the SSS and *E-P* time series covary from 1850 to 2100 over the $E > P$ and the $E < P$ domain, respectively. The color of the filled symbols is model-dependent and depicts the sign and magnitude of the correlation between the global ocean SSS and *E-P* contrasts. The obtained

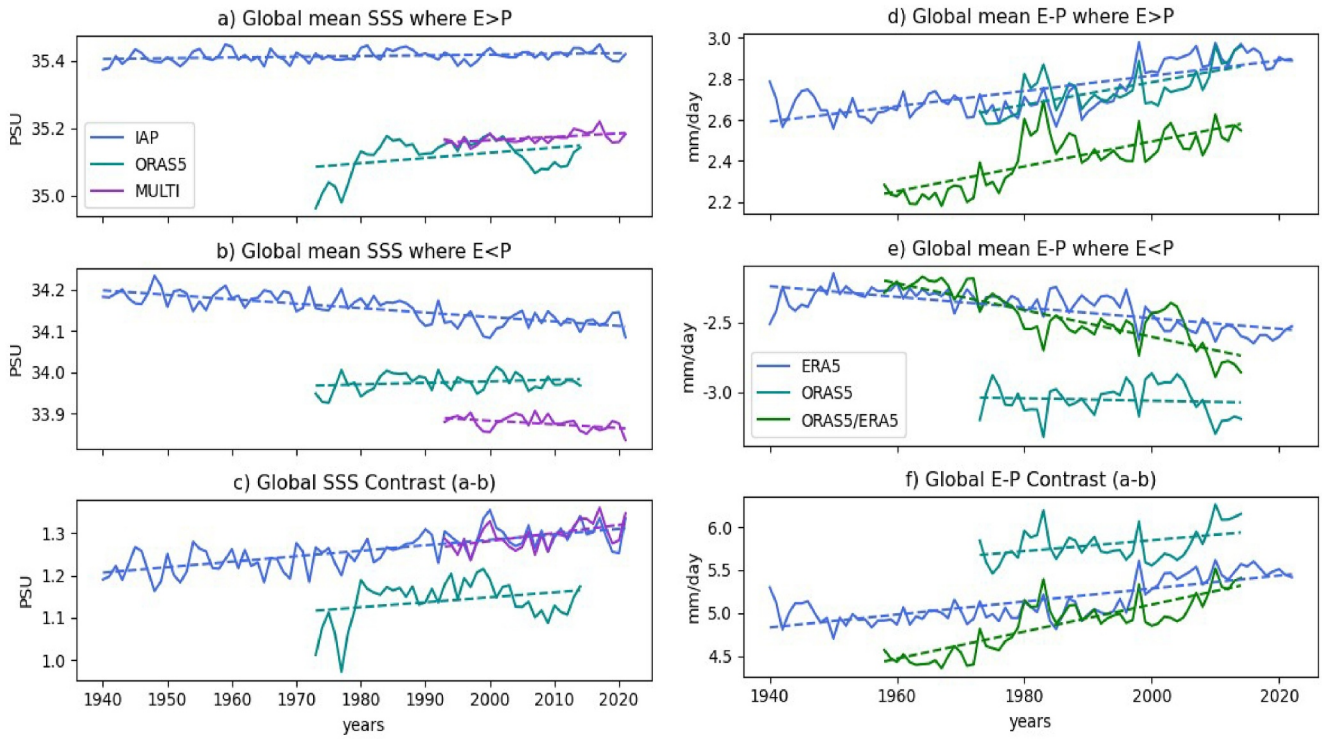

Figure 1. Annual mean timeseries (solid lines) and linear fits (dashed lines) for three global sea surface salinity (PSU, left panels) and *E-P* (mm/day, right panels) data sets spatially averaged over two contrasted global ocean domains where (a) $E > P$ and (b) $E < P$ according to the ERA5 monthly mean reanalysis. Panel (c) is simply the difference between panels (a) and (b) and thus corresponds to our GSSSC index (left panel) or the corresponding *E-P* contrast (right panel). As indicated in the two legends, the different colors do net refer to the same data sets for left versus right panels. Note that the ORAS5 ocean reanalysis has been driven by *E-P* fluxes from former ECMWF reanalyzes (not ERA5) so that ERA5 and ORAS5 timeseries have not been averaged over exactly the same *E-P* domains. As an intermediate estimate, ORAS5/ERA5 is based on *E-P* fluxes from ORAS5 but using the ERA5 dynamic *E-P* mask to distinguish between the $E > P$ and $E < P$ domains (and using the whole 1958–2014 ORAS5 consolidated data, cf. details in Table S1 in Supporting Information S1).

"butterfly pattern" highlights an asymmetric relationship between SSS and *E-P* variations over the $E > P$ versus $E < P$ ocean domains. Even the sign of the correlation remains model-dependent over the $E > P$ domain, thus challenging the robustness of the FFSS paradigm.

Although the year-to-year variability may slightly contribute, the inter-model spread in the correlations is clearly dominated by contrasted linear trends across the full 1850–2100 period. This interpretation is supported by Figure S4 in Supporting Information S1 showing similar scatterplots but for the projected *E-P* versus SSS relative anomalies. Over the $E > P$ domain, all *E-P* anomalies are positive but they are poorly related to the salinity changes which are either negative or positive, in line with the correlations shown in Figure 2. Although both *E-P* and SSS anomalies are all negative over the $E < P$ domain, the relevance of the dipole GSSSC index as a surrogate for the global ocean *E-P* contrast is challenged, at least for the CMIP6 models that do not appear in dark red in Figure 2. This poor link between the *E-P* contrast and corresponding GSSSC anomalies is however the antithesis of the strong scaling of the *E-P* contrast anomalies with the projected global warming (Figure S4d in Supporting Information S1). Such a link does not exist at the regional scale (Elbaum et al., 2022) and even at the global ocean scale when using "static" rather than "dynamic" ocean domains (not shown), thus supporting the relevance of the ocean domain definition when assessing salinity contrasts (e.g., Levang & Schmitt, 2015).

Looking at the global geographical distribution of projected SSS changes, Figure S5 in Supporting Information S1 indicates that the ensemble-mean CMIP6 salinity response is dominated by a North Atlantic dipole which may reflect a projected slowdown of the Atlantic Meridional Overturning Circulation (AMOC) and thus of (heat and) salt transport from the tropics to the extra-tropics. Such an interpretation is at least consistent with a former analysis based on CMIP5 models (Skliris et al., 2020) showing that an AMOC decline can induce a southward shift of the Inter-Tropical Convergence Zone, a dipole pattern of precipitation change over the tropical region and,

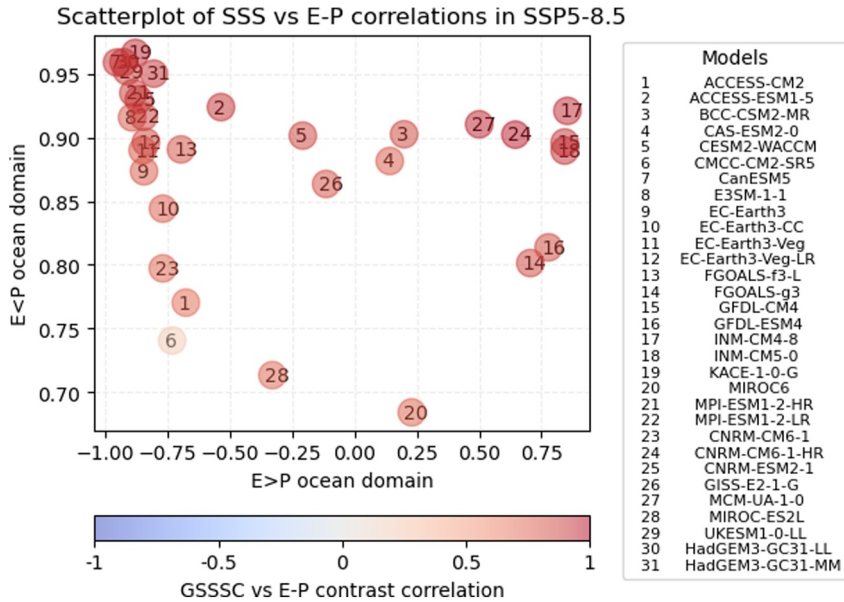

Figure 2. Scatterplot of correlations between annual mean *E-P* and sea surface salinity (SSS) timeseries (1850–2100) from 31 CMIP6 models (only one realization for each model). The correlation is estimated over the $E > P$ ocean domain on the *x*-axis and over the $E < P$ domain on the *y*-axis. The color of the filled circles (one for each CMIP6 model) depicts the correlation between the global SSS and *E-P* contrasts with redish colors for positive values and bluish for negative. All data are raw timeseries without any filtering or smoothing. Yet, the results are fairly similar after removing the interannual variability (not shown) and are fairly robust across different concentration scenarios (Figure S13 in Supporting Information S1).

thus, a decrease in freshwater input north of the equator. Ultimately, this mechanism drives a strong salinification of the subtropics region and strengthens the northward salinity transport in the North Atlantic Ocean basin.

Opposite changes between the tropical Pacific and tropical Atlantic are also found, in line with Terray et al. (2012). Yet, the prominent North Atlantic dipole suggests that this inter-basin SSS contrast may not be the most suitable index to assess the intensification of the water cycle over the global ocean. Moreover, the ensemble mean response conceals considerable modeling uncertainties, as revealed by the standard deviation and local 10th and 90th percentiles of the local SSS changes in Figure S5 in Supporting Information S1. This is no surprise given the considerable modeling uncertainties found in the CMIP6 hydrological projections (Douville et al., 2021), including for precipitation (Figure S6 in Supporting Information S1), surface evaporation (Figure S7 in Supporting Information S1) and, thus, their *P-E* difference (Figure S8 in Supporting Information S1).

Narrowing modeling uncertainty in available climate projections is a fast-growing area of research. Here we use the KCC Bayesian statistical package (KCC, 2023) already applied to multiple variables and domains in both CMIP5 and CMIP6 projections (Douville, 2023; Douville & Willett, 2023; Douville et al., 2022; Qasmi & Ribes, 2022; Ribes et al., 2021). The method was successfully evaluated in idealized settings both at global and regional scales (see also Dutot & Douville, 2023). Compared to linear regression methods, it takes advantage of the full observational record, accounts for uncertainties due to both internal variability and observational errors, and is less sensitive to potential outliers or redundancies in the raw model distribution (Sanderson et al., 2021).

Annual mean GSSSC timeseries have been computed from the monthly mean SSS outputs of 31 CMIP6 models after concatenation of historical (1850–2014) and scenario (2015–2100) simulations (one realization only). The calculation was made after SSS interpolation onto the corresponding native atmospheric grid to apply a model-dependent *E-P* dynamic mask (cf. Equation 1). The focus of KCC is on the forced model response so that internal variability was first removed from all concatenated time series using a spline smoothing with six degrees of freedom. The prior distribution was then estimated assuming a Gaussian distribution of the multi-model ensemble. Finally, the posterior distribution was derived (cf. details in Qasmi & Ribes, 2022) conditional to two independent observed data sets: the 1850–2021 GMST record from HadCRUT (https://www.metoffice.gov.uk/hadobs/hadcrut5/) and the 1940–2021 GSSSC index derived from the IAP reconstruction (G. Li et al., 2023).

KCC allows us to constrain both recent and future climate changes in a consistent way. Here we first apply the method over two 50-year periods: 1951–2000 (as in Durack et al., 2012) and 1972–2021 (as the latest available 50-year observation period), respectively. The first scatterplot (Figure S9a in Supporting Information S1) shows the late 20th change in GSSSC versus the corresponding increase in global mean near-surface air temperature (GSAT). Although the estimated rate of increase in our different GSSSC index, around +6%/°C, is much lower than in Durack et al. (2012) over the same period, the results somehow support their conclusion whereby most (here CMIP6 instead of CMIP3) climate models underestimate the global salinity pattern amplification. Yet, the 5%–95% bivariate confidence interval of the observed amplification and global warming is very large, so that the KCC posterior distribution of the model response, conditional to the observed time series, only shows a limited narrowing of plausible changes. The revised ensemble-mean amplification of salinity patterns is around +3.5%/°C and thus higher than the +2%/°C rate of the prior.

Looking at the more recent 1972–2021 period (Figure S9b in Supporting Information S1), excluding the less reliable early IAP record and closer to the timescale explored by Cheng et al. (2020), the observations show an accelerated global warming and a higher rate of increase in salinity contrast compared to the late 20th century. In line with Ribes et al. (2021), the ensemble-mean recent global warming simulated by the CMIP6 models is too strong, while the simulated GSSSC index becomes more consistent with the IAP best estimate. The CMIP6 ensemble mean rate of amplification of the global salinity pattern amplification is still around +2%/°C and thus lower than the observed estimate. Although the 5–95% confidence interval of the IAP GSSSC change is reduced compared to the late 20th century, the parallel increase in the simulated confidence interval prevents KCC to exert a strong constraint on the projections. Yet, the posterior ensemble mean rate of increase in GSSSC now perfectly matches the observed best guess estimate.

Moving to the transient 1850–2100 climate simulations driven by the high-emission SSP5-8.5 scenario after 2014, Figure 3 shows the constrained versus unconstrained anomalies of the annual mean GSAT and GSSSC indices relative to the 1995–2014 climatology. The upper left panel (Figure 3a) confirms that the ensemble mean global warming is overestimated due to a fraction of over-sensitive CMIP6 models. The observed historical warming from HadCRUT is less effective in constraining the GSSSC projections despite a slight reduction in the projected amplification of the global SSS patterns (Figure 3b). Although the IAP observations also exert a limited constraint (Figure 3c), the combined use of both HadCRUT and IAP observations leads to temper the projected ensemble-mean increase in GSSSC and to narrow the late century 5%–95% confidence interval by about 21% (Figure 3d).

Such a result means that the projected amplification of the global SSS pattern is slightly overestimated by some CMIP6 models. This conclusion is also found when using a static rather than dynamic ERA5 *E-P* mask (Figure S10 in Supporting Information S1). Nevertheless, the two polarities of the dynamic GSSSC index do not show a fully symmetric response after constraint. A stronger narrowing of model uncertainties is found over the $E > P$ ocean domain (Figure S11 in Supporting Information S1) than over the $E < P$ complementary domain (Figure S12 in Supporting Information S1). This is mostly due to the fact that even the sign of the salinity response is model-dependent over the $E > P$ domain where the signal to noise ratio in the IAP observations is moreover limited. As a result, even the posterior distribution does not exclude a decrease in salinity over the $E > P$ subtropical ocean domain.

4. Discussion and Conclusion

The global water cycle is expected to intensify with increasing GMST, as evidenced by the so-called hydrological sensitivity (η) estimated from idealized climate change experiments (Allan et al., 2020; Fläschner et al., 2016). Yet, this simple metric is based on the scaled global mean precipitation response (∼2–3%/°C) and does not tell much about changes in terrestrial water availability. Despite a robust increase of total precipitable water by around 7%/°C (e.g., Douville et al., 2022), projected changes in *P-E* patterns cannot be simply interpreted as a "wet gets wetter, dry gets drier" response (e.g., Byrne & O'Gorman, 2015). Yet, its "FFSS" oceanic counterpart was so far still considered as a valid paradigm for the overall intensification of the global water cycle (Allan et al., 2020; Bindoff et al., 2019; Cheng et al., 2020).

By integrating the synoptic and high-frequency variability of *E-P* fields, SSS changes appear as a suitable proxy for *E-P* changes at the ocean basin scale. Early studies have revealed an enhanced salinity contrast between the freshening Pacific and the increasingly salty Atlantic, which could not be explained by internal climate variability

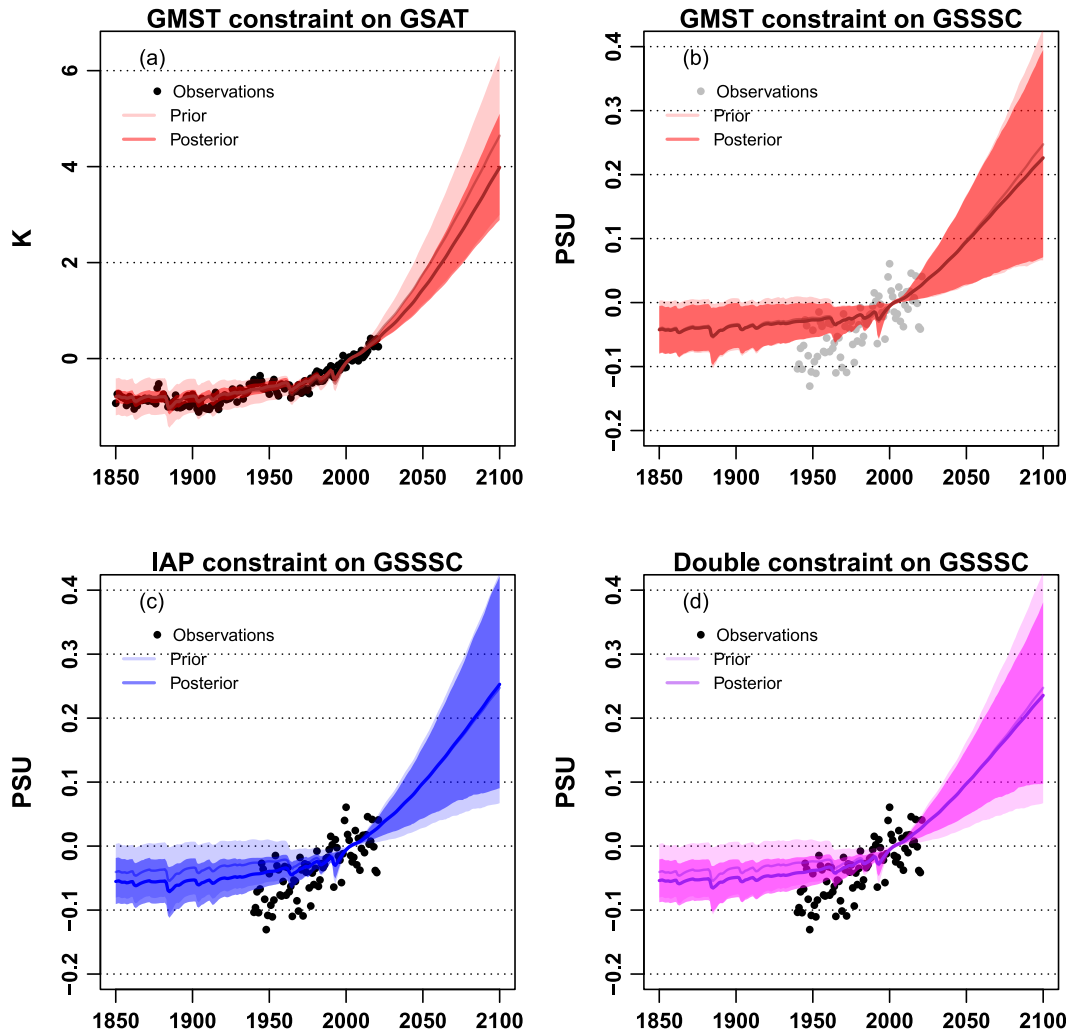

Figure 3. Constrained versus unconstrained annual forced changes in (a) global mean surface temperature (GSAT, K) and (b–d) global sea surface salinity contrast (GSSSC, PSU) derived from 32 CMIP6 models under the SSP5-8.5 high-emission scenario. Mean (solid lines) and 5%–95% range (shading) of the prior and posterior distributions of the GSAT and GSSSC response to both natural and anthropogenic radiative forcings from 1850 to 2100 (all anomalies are relative to the 1995–2014 climatology). (a) HadCRUT-only observational constraint on GSAT; (b) HadCRUT-only observational constraint on GSSSC; (c) IAP-only observational constraint on GSSSC; (d) HadCRUT and Institute of Atmospheric Physics observational constraints on GSSSC. After the constraint, the 5%–95% interval at the end of the 21st century is reduced by 33.2%, 8.6%, 10.2%, and 21.4% in panel (a–d) respectively. The annual mean observed anomalies are shown as black (gray) filled circles when they are (not) used for constraining the model response.

(e.g., Terray et al., 2012). Such a growing inter-basin contrast is further supported by the IAP data set (Figure S13 in Supporting Information S1) and a recent multi-model study (Sun & Du, 2022). Other parallel studies, based on zonal mean and basin-dependent indices, also revealed a human contribution to observed changes in salinity contrasts (Durack et al., 2012; Pierce et al., 2012). Yet, the link with water cycle intensity may not be a constant property of the climate system (e.g., Cheng et al., 2020) and may be sensitive to the selected ocean domains.

Our study is based on ad hoc ocean domains, separated by the $E = P$ isoline, rather than by absolute salinity thresholds. They however confirm a long-term amplification of the climatological SSS patterns. The relevance of the selected domains is supported by the high inter-model correlation between the projected E-P changes over the $E > P$ and $E < P$ respectively (Figure S3b in Supporting Information S1). Yet, the "butterfly pattern" shown in Figure 2 highlights that the "salty gets saltier" mechanism may not be operating in all models. This feature is also found in a lower emission scenario (cf. Figure S13 in Supporting Information S1). It highlights the sensitivity of the FFSS paradigm to the ocean contrast definition and it challenges here the possibility to assess water cycle

intensity from the SSS contrast, at least for the few CMIP6 models that do not show a strong correspondence between *E-P* and SSS changes respectively in Figure 2 (and Figure S14 in Supporting Information S1).

A detailed explanation of the asymmetric salinity response is beyond the scope of the present study. Preliminary analyses suggest that the 10 CMIP6 models that fully support the FFSS paradigm show a stronger SSS increase over the tropical Pacific associated with an enhanced salinity dipole over the North Atlantic, compared to the other CMIP6 models (Figure S15a in Supporting Information S1). Overall, this subset of models also shows a weaker surface ocean warming, which may dilute the increase in GSSSC through a lower stratification (Zika et al., 2018). This relative cooling is however not uniform and shows a more symmetric (i.e., less Niño-like) tropical Pacific warming (Figure S15b in Supporting Information S1), and thus less divergence (i.e., negative *E-P* differences in Figure S15c in Supporting Information S1) and more precipitation (Figure S15d in Supporting Information S1) over the western Pacific. These results may be consistent with a tropical Pacific forcing of a positive AMOC response via tropical-extratropical teleconnections (Orihuela-Pinto et al., 2023), associated with a global cooling (Bonnet et al., 2021) and a transient tropical SST pattern (e.g., Andrews et al., 2022).

Beyond the indirect assessment of water cycle intensification, more reliable estimates of salinity changes may also contribute to a better understanding of the human influence on the ocean system itself. Salinity changes represent both a potential driver and tracer of the AMOC (e.g., Bonan et al., 2022). In the high latitudes, the dominant "fresh gets fresher" mechanism tends to enhance the ocean stratification and, thus, the magnitude of the surface ocean warming (e.g., G. C. Li et al., 2020; Yamaguchi & Suga, 2019). The decrease in upper ocean salinity projected in the Arctic however remains highly uncertain (e.g., Khosravi et al., 2022). Future studies should also focus on the projected changes in ocean transport and upper ocean stratification (e.g., Olmedo et al., 2022) and their possible influence on global SSS contrasts and on the simulated transfer functions between salinity and *E-P* changes.

Data Availability Statement

All model outputs from the CMIP6 historical and scenario experiments are freely accessible at https://pcmdi.llnl.gov/CMIP6/ or at https://esgf-node.llnl.gov/projects/esgf-llnl/. All salinity datasets listed in Table S1 in Supporting Information S1 and in the reference list are freely accessible, including IAP from G. Li et al. (2023), Copernicus Climate Change Service (2023), and Copernicus Marine Service (2023). All graphics have been produced using the R or Matplotlib software freely accessible at https://cran.r-project.org/ and https://matplotlib.org/ respectively.

Acknowledgments
The authors are grateful for the insightful comments from the editor and two anonymous reviewers that help improve the paper greatly. Thanks are also due to all CMIP6 participants and to Sarah Berthet, Aurélien Ribes, Jean-Baptiste Sallée and Laurent Terray for helpful discussions about the early manuscript.

References

Allan, R. P., Barlow, M., Byrne, M. P., Cherchi, A., Douville, H., Fowler, H. J., et al. (2020). Advances in understanding large-scale responses of the water cycle to climate change. *Annals of the New York Academy of Sciences*, *1472*, 1–27. https://doi.org/10.1111/nyas.14337

Andrews, T., Bodas-Salcedo, A., Gregory, J. M., Dong, Y., Armour, K. C., Paynter, D., et al. (2022). On the effect of historical SST patterns on radiative feedback. *Journal of Geophysical Research: Atmospheres*, *127*(18), e2022JD036675. https://doi.org/10.1029/2022JD036675

Bindoff, N. L., Cheung, W. W., Kairo, J. G., Arístegui, J., Guinder, V. A., Hallberg, R., et al. (2019). Changing ocean, marine ecosystems, and dependent communities. In H.-O. Pörtner, D. C. Roberts, V. Masson-Delmotte, P. Zhai, M. Tignor, E. Poloczanska, et al. (Eds.), *IPCC special report on the ocean and cryosphere in a changing climate* (pp. 447–587). Cambridge University Press. https://doi.org/10.1017/9781009157964.007

Bonan, D. B., Thompson, A. F., Newsom, E. R., Sun, S., & Rugenstein, M. (2022). Transient and equilibrium responses of the Atlantic overturning circulation to warming in coupled climate models: The role of temperature and salinity. *Journal of Climate*, *35*(15), 5173–5191. https://doi.org/10.1175/jcli-d-21-0912.1

Bonnet, R., Swingedouw, D., Gastineau, G., Boucher, O., Deshayes, J., Hourdin, F., et al. (2021). Increased risk of near term global warming due to a recent AMOC weakening. *Nature Communications*, *12*(1), 6108. https://doi.org/10.1038/s41467-021-26370-0

Byrne, M. P., & O'Gorman, P. A. (2015). The response of precipitation minus evapotranspiration to climate warming: Why the "Wet-Get-Wetter, dry-get-drier" scaling does not hold over land. *Journal of Climate*, *28*(20), 8078–8092. https://doi.org/10.1175/jcli-d-15-0369.1

Cheng, L., Trenberth, K. E., Gruber, N., Abraham, J. P., Fasullo, J., Li, G., et al. (2020). Improved estimates of changes in upper Ocean Salinity and the hydrological cycle. *Journal of Climate*, *33*(23), 10357–10381. https://doi.org/10.1175/jcli-d-20-0366.1

Copernicus Climate Change Service. (2023). ORAS5 global ocean reanalysis monthly data from 1958 to present [Dataset]. *Copernicus Climate Change Service (C3S) Climate Data Store (CDS)*. https://doi.org/10.24381/cds.67e8eeb7

Copernicus Marine Service. (2023). Multi observation Global Ocean sea surface salinity and sea surface density [Dataset]. *Copernicus Marine Service*. https://doi.org/10.48670/moi-00051

Douville, H. (2023). Robust and perfectible constraints on human-induced Arctic climate change. *Communications Earth & Environment*, *4*(1), 283. https://doi.org/10.1038/s43247-023-00949-5

Douville, H., Raghavan, K., Renwick, J., Allan, R. P., Arias, P. A., Barlow, M., et al. (2021). Water cycle changes. In V. Masson-Delmotte, P. Zhai, A. Pirani, S. L. Connors, C. Péan, S. Berger, et al. (Eds.), *Climate change 2021: The physical science basis. Contribution of working*

group I to the sixth assessment report of the intergovernmental panel on climate change (pp. 1055–1210). Cambridge University Press. https://doi.org/10.1017/9781009157896.010

Douville, H., Ribes, A., & Bock, O. (2022). Global warming at near-constant relative humidity further supported by recent in situ observations. *Communications Earth & Environment*, *3*(1), 237. https://doi.org/10.1038/s43247-022-00561-z

Douville, H., & Willett, K. (2023). A drier than expected future, supported by near-surface relative humidity observations. *Science Advances*, *9*(30), eade6253. https://doi.org/10.1126/sciadv.ade6253

Durack, P. J., Wijffels, S. E., & Matear, R. J. (2012). Ocean salinities reveal strong global water cycle intensification during 1950 to 2000. *Science*, *336*(6080), 455–458. https://doi.org/10.1126/science.1212222

Dutot, E., & Douville, H. (2023). Revisiting the potential to narrow uncertainty in annual runoff projections of Arctic rivers. *Geophysical Research Letters*, *50*(16), e2023GL104039. https://doi.org/10.1029/2023GL104039

Elbaum, E., Garfinkel, C. I., Adam, O., Morin, E., Rostkier-Edelstein, D., & Dayan, U. (2022). Uncertainty in projected changes in precipitation minus evaporation: Dominant role of dynamic circulation changes and weak role for thermodynamic changes. *Geophysical Research Letters*, *49*(12), e2022GL097725. https://doi.org/10.1029/2022GL097725

Fläschner, D., Mauritsen, T., & Stevens, B. (2016). Understanding the intermodel spread in global-mean hydrological sensitivity. *Journal of Climate*, *29*(2), 801–817. https://doi.org/10.1175/JCLI-D-15-0351.1

Grist, J. P., Josey, S. A., Zika, J. D., Evans, D. G., & Skliris, N. (2016). Assessing recent air-sea freshwaterflux changes using a surface temperature-salinity space framework. *Journal of Geophysical Research: Oceans*, *121*(12), 8787–8806. https://doi.org/10.1002/2016JC012091

Hersbach, H., Bell, B., Berrisford, P., Biavati, G., Horányi, A., Muñoz Sabater, J., et al. (2020). The ERA5 global reanalysis. *Quarterly Journal of the Royal Meteorological Society*, *146*(730), 1999–2049. https://doi.org/10.1002/qj.3803

Hersbach, H., Bell, B., Berrisford, P., Biavati, G., Horányi, A., Muñoz Sabater, J., et al. (2023). ERA5 monthly averaged data on single levels from 1940 to present [Dataset]. *Copernicus Climate Change Service (C3S) Climate Data Store (CDS)*. https://doi.org/10.24381/cds.f17050d7

KCC. (2023). Kriging for climate change [Software]. *GNU General Public License, version 3 (GPLv3)*. https://doi.org/10.5281/zenodo.5233947

Khosravi, N., Wang, Q., Koldunov, N., Hinrichs, C., Semmler, T., Danilov, S., & Jung, T. (2022). The Arctic Ocean in CMIP6 models: Biases and projected changes in temperature and salinity. *Earth's Future*, *10*(2), e2021EF002282. https://doi.org/10.1029/2021EF002282

Lehner, F., Deser, C., Maher, N., Marotzke, J., Fischer, E., Brunner, L., et al. (2020). Partitioning climate projection uncertainty with multiple large ensembles and CMIP5/6. *Earth System Dynamics*. https://doi.org/10.5194/esd-2019-93

Levang, S. J., & Schmitt, R. W. (2015). Centennial changes of the global water cycle in CMIP5 models. *Journal of Climate*, *28*(16), 6489–6502. https://doi.org/10.1175/JCLI-D-15-0143.1

Li, G., Cheng, L., Pan, G., Wang, H., Liu, J., Zhu, B., et al. (2023). A global gridded ocean salinity dataset with 0.5° horizontal resolution since 1960 for the upper 2000 m [Dataset]. *Frontiers in Marine Science*, *10*, 1108919. https://doi.org/10.3389/fmars.2023.1108919

Li, G. C., Cheng, L. J., Zhu, J., Trenberth, K. E., Mann, M. E., & Abraham, J. P. (2020). Increasing ocean stratification over the past half-century. *Nature Climate Change*, *10*(12), 1116–1123. https://doi.org/10.1038/s41558-020-00918-2

Liu, C., Liang, X., Chambers, D. P., & Ponte, R. M. (2020). Global patterns of spatial and temporal variability in salinity from multiple gridded argo products. *Journal of Climate*, *33*(20), 8751–8766. https://doi.org/10.1175/JCLI-D-20-0053.1

Liu, Y., Cheng, L., Pan, Y., Tan, Z., Abraham, J., Zhang, B., et al. (2022). How well do CMIP6 and CMIP5 models simulate the climatological seasonal variations in ocean salinity? *Advances in Atmospheric Sciences*, *39*(10), 1650–1672. https://doi.org/10.1007/s00376-022-1381-2

Mayer, J., Mayer, M., & Haimberger, L. (2021). Consistency and homogeneity of atmospheric Energy, moisture, and mass budgets in ERA5. *Journal of Climate*, *34*(10), 3955–3974. https://doi.org/10.1175/jcli-d-20-0676.1

Olmedo, E., Turriel, A., González-Gambau, V., González-Haro, C., García-Espriu, A., Gabarró, C., et al. (2022). Increasing stratification as observed by satellite sea surface salinity measurements. *Scientific Reports*, *12*(1), 6279. https://doi.org/10.1038/s41598-022-10265-1

Orihuela-Pinto, B., Santoso, A., England, M. H., & Taschetto, A. S. (2023). Coupled feedbacks from the tropical Pacific to the Atlantic meridional overturning circulation. *Geophysical Research Letters*, *50*(20), e2023GL103250. https://doi.org/10.1029/2023GL103250

Pierce, D. W., Gleckler, P. J., Barnett, T. P., Santer, B. D., & Durack, P. J. (2012). The fingerprint of human-induced changes in the ocean's salinity and temperature fields. *Geophysical Research Letters*, *39*(21), L21704. https://doi.org/10.1029/2012GL053389

Qasmi, S., & Ribes, A. (2022). Reducing uncertainty in local climate projections. *Science Advances*, *8*, eabo6872. https://doi.org/10.1126/sciadv.abo6872

Ribes, A., Qasmi, S., & Gillett, N. (2021). Making climate projections conditional on historical observations. *Science Advances*, *7*(4), eabc0671. https://doi.org/10.1126/sciadv.abc0671

Robertson, F. R., Bosilovich, M. G., & Roberts, J. B. (2016). Reconciling land–ocean moisture transport variability in reanalyses with P-ET in observationally driven land surface models. *Journal of Climate*, *29*(23), 8625–8646. https://doi.org/10.1175/jcli-d-16-0379.1

Sanderson, B. M., Pendergrass, A. G., Koven, C. D., Brient, F., Booth, B. B. B., Fisher, R. A., & Knutti, R. (2021). The potential for structural errors in emergent constraints. *Earth System Dynamics*, *12*(3), 899–918. https://doi.org/10.5194/esd-12-899-2021

Shi, L., Alves, O., Wedd, R., Balmaseda, M. A., Chang, Y., Chepurin, G., et al. (2017). An assessment of upper ocean salinity content from the Ocean Reanalyses Inter-comparison Project (ORA-IP). *Climate Dynamics*, *49*(3), 1009–1029. https://doi.org/10.1007/s00382-015-2868-7

Skliris, N., Marsh, R., Mecking, J. V., & Zika, J. D. (2020). Changing water cycle and freshwater transports in the Atlantic Ocean in observations and CMIP5 models. *Climate Dynamics*, *54*(11–12), 4971–4989. https://doi.org/10.1007/s00382-020-05261-y

Skliris, N., Zika, J. D., Nurser, G., Josey, S. A., & Marsh, R. (2016). Global water cycle amplifying at less than the Clausius-Clapeyron rate. *Scientific Reports*, *6*(1), 38752. https://doi.org/10.1038/srep38752

Sun, Q., & Du, Y. (2022). Sea surface salinity changes in response to El Niño-like SST warming and relevant ocean dynamics in the tropical Pacific under the CMIP6 abrupt-4XCO_2 scenario. *Journal of Climate*, *35*(18), 5839–5854. https://doi.org/10.1175/JCLI-D-21-0973.1

Terray, L., Corre, L., Cravatte, S., Delcroix, T., Reverdin, G., & Ribes, A. (2012). Near-surface salinity as Nature's rain gauge to detect human influence on the tropical water cycle. *Journal of Climate*, *25*(3), 958–977. https://doi.org/10.1175/jcli-d-10-05025.1

Vinogradova, N. T., & Ponte, R. M. (2013). Clarifying the link between surface salinity and freshwater fluxes on monthly to interannual time scales. *Journal of Geophysical Research: Oceans*, *118*(6), 3190–3201. https://doi.org/10.1002/jgrc.20200

Wang, H., You, Z., Guo, H., Zhang, W., Xu, P., & Ren, K. (2023). Quality assessment of sea surface salinity from multiple ocean reanalysis products. *Journal of Marine Science and Engineering*, *11*(1), 54. https://doi.org/10.3390/jmse11010054

Yamaguchi, R., & Suga, T. (2019). Trend and variability in global upper-ocean stratification since the 1960s. *Journal of Geophysical Research: Oceans*, *124*(12), 8933–8948. https://doi.org/10.1029/2019jc015439

Yu, L., Jin, X., Josey, S. A., Lee, T., Kumar, A., Wen, C., & Xue, Y. (2017). The global ocean water cycle in atmospheric reanalysis, satellite, and ocean salinity. *Journal of Climate*, *97*(10), 3829–3852. https://doi.org/10.1175/jcli-d-16-0479.1

Yu, L., Josey, S. A., Bingham, F., & Lee, T. (2017). Intensification of the global water cycle and evidence from ocean salinity: A synthesis review. *Annals of the New York Academy of Sciences*, *1472*(1), 76–94. https://doi.org/10.1111/nyas.14354

Zika, J. D., Skliris, N., Blaker, T. A., Marsh, R., Nurser, A. J. G., & Josey, S. A. (2018). Improved estimates of water cycle change from ocean salinity: The key role of ocean warming. *Environmental Research Letters*, *13*(7), 074036. https://doi.org/10.1088/1748-9326/aace42

Zuo, H., Balmaseda, M. A., Tietsche, S., Mogensen, K., & Mayer, M. (2019). The ECMWF operational ensemble reanalysis–analysis system for ocean and sea ice: A description of the system and assessment. *Ocean Science*, *15*(3), 779–808. https://doi.org/10.5194/os-15-779-2019